3-2013

Tuning Photophysical Properties And Improving Nonlinear Absorption Of Pt(ii) Diimine Complexes With Extended Pi-conjugation In The Acetylide Ligands

Rui Liu

Alexander Azenkeng

Dapeng Zhou

Yuhao Li

Ksenija D. Glusac
Bowling Green State University - Main Campus, kglusac@bgsu.edu

See next page for additional authors

THE JOURNAL OF PHYSICAL CHEMISTRY A

Article

pubs.acs.org/JPCA

Tuning Photophysical Properties and Improving Nonlinear Absorption of Pt(II) Diimine Complexes with Extended π-Conjugation in the Acetylide Ligands

Rui Liu,[†] Alexander Azenkeng,[‡] Dapeng Zhou,[§] Yuhao Li,[†] Ksenija D. Glusac,[§] and Wenfang Sun*[,†]

[†]Department of Chemistry and Biochemistry, North Dakota State University, Fargo, North Dakota 58108-6050, United States

[‡]Energy and Environmental Research Center, University of North Dakota, Grand Forks, North Dakota 58202-9018, United States

[§]Department of Chemistry, Bowling Green State University, Bowling Green, Ohio 43403-0001, United States

Supporting Information

ABSTRACT: Two new Pt(II) 4,4′-di(5,9-diethyltridecan-7-yl)-2,2′-bipyridine complexes (**1** and **2**) bearing 9,9-diethyl-2-ethynyl-7-(2-(4-nitrophenyl)-ethynyl)-9*H*-fluorene ligand and *N*-(4-(2-(9,9-diethyl-7-ethynyl-9*H*-fluoren-2-yl)ethynyl)phenyl)-*N*-phenylbenzeneamine ligand, respectively, were synthesized and characterized. Their photophysical properties were investigated systematically by UV−vis absorption, emission, and transient absorption (TA) spectroscopy, and the nonlinear absorption was studied by nonlinear transmission technique. Theoretical TD-DFT calculations using the CAM-B3LYP functional were carried out to determine the nature of the singlet excited electronic states and to assist in the assignment of significant transitions observed in experiments. Complex **1** exhibits an intense, structureless absorption band at ca. 397 nm in CH_2Cl_2 solution, which is attributed to mixed metal-to-ligand charge transfer (^{1}MLCT)/ligand-to-ligand charge transfer (^{1}LLCT)/intraligand charge transfer (^{1}ILCT)/$^1\pi,\pi^*$ transitions, and two ^{1}MLCT/^{1}LLCT transitions in the 300−350 nm spectral region. Complex **2** possesses an intense acetylide ligand localized $^1\pi,\pi^*$ absorption band at ca. 373 nm and a moderately intense ^{1}MLCT/^{1}LLCT tail above 425 nm in CH_2Cl_2. Both complexes are emissive in solution at room temperature, with the emitting state being tentatively assigned to the predominant $^3\pi,\pi^*$ state for **1**, whereas the emitting state of **2** exhibits a switch from $^3\pi,\pi^*$ state in high-polarity solvents to ^{3}MLCT/^{3}LLCT state in low-polarity solvents. Both **1** and **2** exhibit strong singlet excited-state TA in the visible to NIR region, where reverse saturable absorption (RSA) is feasible. The spectroscopic studies and theoretical calculations indicate that the photophysical properties of these Pt complexes can be tuned drastically by extending the π-conjugation of the acetylide ligands. In addition, strong RSA was observed at 532 nm for nanosecond (ns) laser pulses from **1** and **2**, demonstrating that the RSA of the Pt(II) diimine complexes can be improved by extending the π-conjugation of the acetylide ligands.

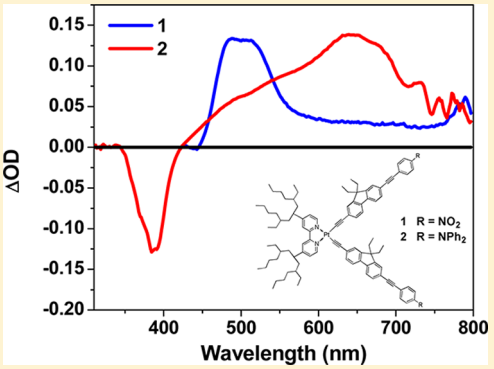

INTRODUCTION

Pt(II) diimine bisacetylide complexes[1] are interesting photofunctional materials. They have shown potential applications in a variety of photonic processes and devices, such as solar energy conversion via photoinduced charge separation,[2−4] low-power upconversion,[5−9] luminescent materials,[10−12] chemosensors,[13,14] and nonlinear optics.[15−17] These applications are primarily based on the square-planar configuration and the rich photophysical properties of the Pt(II) diimine complexes, which can be readily tuned by structural modifications to meet the specific requirements for a predetermined application.

It has been reported that the lowest-energy absorption band(s) in many of the Pt(II) diimine complexes is the metal-to-ligand charge transfer (^{1}MLCT)/ligand-to-ligand charge transfer (^{1}LLCT) absorption band(s), which can be tuned by the substituent on the bipyridine ligand or on the acetylide ligands.[18−20] Although the effect of the substituents on the bipyridine ligand is well understood, no monotonic trend was observed on the emission energy, lifetime, and quantum yield upon variation of the substituents on the acetylide ligands. The latter phenomenon is attributed to the admixture or switching order of multiple excited states in proximity. Our group recently reported the influence of the auxiliary substituent on the photophysics of Pt(II) bipyridyl bisfluorenylacetylide complexes[21] and Pt(II) bipyridyl bisstilbenylacetylide complexes,[22] respectively. When a strong electron-withdrawing substituent is introduced to the acetylide ligand, the lowest singlet and triplet excited states of the Pt(II) bipyridyl complex are dominated by the acetylide ligand localized π,π^* transitions, resulting in long-lived triplet excited state and broadband triplet excited-state absorption.[21,22] Castellano and co-workers[23,24] discovered that when the π-conjugation of the acetylide ligand

Received: October 4, 2012
Revised: February 8, 2013
Published: February 11, 2013

Scheme 1. Structures of Pt(II) Complexes 1−4 and Ligands 1L and 2L

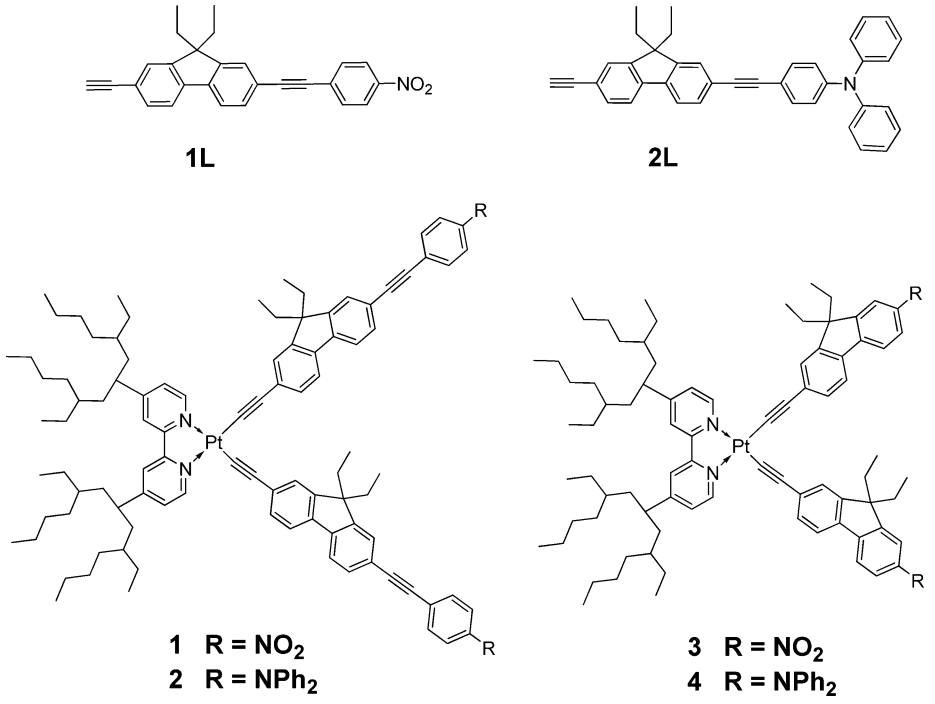

Scheme 2. Synthetic Route for Complexes 1 and 2

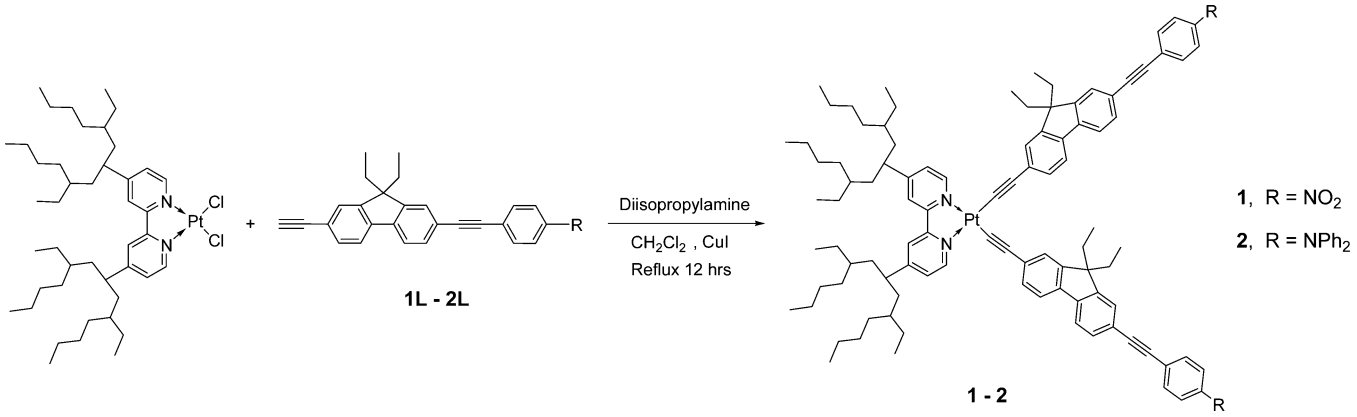

is extended, the contribution of acetylide ligand localized $^3\pi,\pi^*$ state to the lowest triplet excited state becomes more significant, and the configurational mixing and triplet excited-state inversion can be induced by solvent with different polarity. Zhao and co-workers also demonstrated that extending the π-conjugation of the acetylide ligand in Pt(II) diimine complexes led to long-lived acetylide ligand localized $^3\pi,\pi^*$ state and one of the complexes is suitable for triplet−triplet-annihilation based upconversion application.[9] Very recently, our group revealed that when a strong electron-withdrawing aromatic substituent naphthalimide was introduced to the fluorenylacetylide ligand, the lowest singlet and triplet excited states were dominated by the intraligand charge transfer (ILCT) characters in CH_2Cl_2.[25] Moreover, the triplet excited-state lifetimes of these complexes become very long and their reverse saturable absorption is significantly enhanced due to the extended π-conjugation in the acetylide ligand.

On the other hand, our previous studies on the Pt(II) bipyridyl bisfluorenylacetylide complexes[21] and Pt(II) bipyridyl bisstilbenylacetylide complexes[22] manifested that when a strong electron-donating diphenylamino substituent was introduced to the acetylide ligand, both the singlet and triplet excited-states of the resultant Pt(II) complexes absorb strongly in the visible spectral region with $\lambda_{max} \approx 520$ nm, resulting in remarkably strong reverse saturable absorption at 532 nm.

Considering these exciting results and the effect of extended π-conjugation of the acetylide ligand, we envision that extending the π-conjugation of the acetylide ligands in Pt(II) diimine bisfluorenylacetylide complexes with nitro or diphenylamino substituents would prolong the triplet excited state lifetime and further improve their reverse saturable absorption.

With these considerations in mind, two Pt(II) bipyridyl complexes (complex **1** and **2** in Scheme 1) with terminal NO_2 or NPh_2 substituent on the acetylide ligand were synthesized. In order to reduce the intermolecular aggregation and consequently improve the solubility of the Pt(II) complexes, branched alkyl chains were introduced on bipyridine ligand. Complexes **3** and **4** (Scheme 1) have been reported previously by our group[21] and are included in this paper as references for better understanding of the effect of extended π-conjugation.

dx.doi.org/10.1021/jp309841x | J. Phys. Chem. A 2013, 117, 1907−1917

The singlet and triplet excited-state characteristics of **1** and **2** are systematically investigated via UV−vis absorption, steady-state emission, and TA techniques and TD-DFT calculations. The influence on RSA has been demonstrated by nonlinear transmission at 532 nm using ns laser pulses.

EXPERIMENTAL SECTION

Synthesis. The synthetic route for complexes **1** and **2** is provided in Scheme 2. The synthesis and characterization of **3** and **4** were reported by our group previously.[21] All reagents and solvents for synthesis were purchased from Aldrich or Alfa Aesar and used as received. The precursor complex 4,4′-di(5,9-diethyltridecan-7-yl)-2,2′-bipyridyl Pt(II) dichloride (Pt(ddtbpy)Cl_2),[22] ligand **1L**[26] and **2L**[26] were prepared according to literature procedures. All HPLC grade solvents used for spectroscopic studies were purchased from VWR International and used without further purification unless otherwise stated. Silica gels used for chromatography were purchased from Sorbent Technology (230−400 mesh). Complexes **1** and **2** were characterized by ^{1}H NMR and elemental analyses. ^{1}H NMR spectra were obtained on a Varian Oxford-400 VNMR spectrometer or a Varian Oxford-500 VNMR spectrometer. Elemental analyses were carried out by NuMega Resonance Laboratories, Inc. in San Diego, California. HRMS data for **1** and **2** were not obtained due to the difficulty in ionizing the complexes.

General Procedure for Synthesis of Complexes 1 and 2. The ligand **1L** or **2L** (0.70 mmol) and Pt(ddtbpy)Cl_2 (0.33 mmol) were dissolved in degassed mixture of dry CH_2Cl_2 (30 mL) and diisopropyl amine (20 mL). The catalyst CuI (∼5 mg) was then added. The reaction mixture was refluxed under argon for 12 h. After cooling to room temperature, the reaction solution was washed with brine and dried with $MgSO_4$ and the solvent was removed. The residual solid was purified by column chromatography on silica gel using CH_2Cl_2 as the eluent. The product was further purified by recrystallization from CH_2Cl_2 and hexane to yield desired product.

Complex 1. A total of 332 mg of yellow solid was obtained (yield: 63%). ^{1}H NMR (400 MHz, $CDCl_3$) δ 9.84 (d, J = 5.5 Hz, 2H), 7.73 (s, 2H), 7.67 (d, J = 8.0 Hz, 2H), 7.62−7.56 (m, 6H), 7.45 (d, J = 4.5 Hz, 2H), 7.33−7.30 (m, 4H), 7.28−7.25 (m, 2H), 2.95 (br, 2H), 2.09−1.98 (m, 8H), 1.62−1.56 (m, 12H), 1.33−1.09 (m, 36H), 0.93−0.80 (m, 22H), 0.36−0.33 (m, 10H). Anal. Calcd. (%) for $C_{82}H_{110}N_2Pt\cdot{}^1/_3CH_2Cl_2$: C, 73.40; H, 8.30; N, 2.08. Found: C, 73.21; H, 8.37; N, 2.35.

Complex 2. A total of 261 mg of yellow solid was obtained (yield: 43%). ^{1}H NMR (400 MHz, $CDCl_3$) δ 9.77 (d, J = 6.0 Hz, 2H), 7.68 (s, 2H), 7.59−7.51 (m, 8H), 7.45−7.36 (m, 10H), 7.27−7.34 (m, 8H), 7.09 (d, J = 7.6 Hz, 8H), 7.05−6.98 (m, 8H), 2.91 (sh, 2H), 2.03−1.98 (m, 8H), 1.57 (sh, 8H), 1.34−1.05 (m, 36H), 0.82−0.75 (m, 24H), 0.31 (t, J = 7.4 Hz, 12H). Anal. Calcd (%) for $C_{122}H_{136}N_6Pt$: C, 79.06; H, 7.40; N, 3.02. Found: C, 79.07; H, 7.57; N, 2.97.

DFT Calculations. The ground electronic states of complexes **1** and **2** were simulated by density functional theory (DFT) and their excited singlet electronic states were calculated using the time-dependent DFT (TDDFT) method to simulate their theoretical UV−vis absorption spectra. The specific DFT methods used include Becke's exchange (B3) functional, in conjunction with Lee−Yang−Parr (LYP) correlation functional, commonly known as the B3LYP method[27,28] and the Coulomb attenuating model (CAM) modified version of the B3LYP method (CAM-B3LYP) developed by Handy and co-workers.[29] The B3LYP method was used for geometry optimizations, and the CAM-B3LYP method was used for calculating excited electronic states transition energies. The CAM-B3LYP method is one of the recently developed DFT functionals that takes into account the long-range correction effects often encountered in the calculation of charge transfer molecules such as those involved in this work. The basis sets used in all calculations includes functions from the 6-31G* set[30−34] used to describe all light element atoms and the LANL2DZ set[35−37] for the Pt atom; the particular combination is abbreviated in this work as LANG631. LANL2DZ is an effective core potential (ECP) basis set, which was used to provide some corrections for the scalar relativistic effects of the Pt atom.

Full equilibrium geometry optimizations were performed for the ground electronic states of all complexes using a tightened self-consistent field (SCF) convergence threshold of 10^{-9} a.u. To simplify the calculatuions on these large complexes, methyl groups were used to replace the branched alkyl chains on the bipyridine ligand and on the fluorenyl components in complexes **1** and **2**.

Excited state calculations were performed at the fully optimized ground state molecular geometry of the complexes. In addition, bulk solvent effects have been included in all calculations using the polarizable continuum model (PCM).[38] For consistency with experiments, dichloromethane (CH_2Cl_2) that was used as the solvent for experimental measurements was selected as the solvent in theoretical calculations as well. All calculations were performed using the Gaussian 09 (Revision A.1) software suite[39] running on a 96-node distributed-memory cluster with 192 Dual 3.06 GHz Xeon-HT processors at North Dakota State University.

Photophysical Measurements. Ground-state UV−vis absorption spectra of Pt complexes and ligands were measured in a 1 cm quartz cuvette on a Shimadzu UV-2501 spectrophotometer in different solvents (HPLC grade). The steady-state emission spectra were carried out using a HORIBA FluoroMax 4 fluorometer/phosphorometer. Relative actinometry method[40] was applied to measure the emission quantum yields in degassed solutions. A degassed aqueous solution of $[Ru(bpy)_3]Cl_2$ (Φ_{em} = 0.042, λ_{ex} = 436 nm)[41] was used as the reference for Pt complexes and an aqueous solution of quinine bissulfate (Φ_{em} = 0.546, λ_{ex} = 365 nm)[42] was used as the reference for ligands.

The femtosecond (fs) TA spectra and the singlet excited-state lifetimes were measured using a fs pump−probe UV−vis spectrometer. The laser system for the ultrafast TA measurement was described previously.[43] The laser system output consists of a Ti:sapphire oscillator/regenerative amplifier (Hurricane, Spectra Physics) as a source of 800 nm light with full width at half-maximum (fwhm) of 110 fs operating at a repetition rate of 1 kHz. The 800 nm light was split into pump (85%) and probe (10%) beams. The probe beam (800 nm) was delayed by a delay stage (MM4000, Newport). A white light continuum probe beam was produced using a CaF_2 crystal. The sample solution in a 2-mm flow cell was excited using 400 nm light (∼ 2 μJ/pulse) produced by a second harmonic generator (Super Tripler, CSK).

The ns TA spectra, triplet excited-state lifetimes, and triplet excited-state quantum yields were measured on an Edinburgh LP920 laser flash photolysis spectrometer. The excitation source was the third harmonic output (355 nm) of a Nd:YAG laser (Quantel Brilliant, pulsewidth ∼4.1 ns, 1 Hz). Before each

dx.doi.org/10.1021/jp309841x | J. Phys. Chem. A 2013, 117, 1907−1917

measurement, all of the sample solutions were degassed with Ar for 30 min.

The triplet excited-state molar extinction coefficients (ε_T) at the TA band maximum was determined by singlet depletion method,[44] in which ε_T was calculated by the following equation:[44]

$$\varepsilon_T = \frac{\varepsilon_S[\Delta OD_T]}{\Delta OD_S}$$

where ε_S is the ground-state molar extinction coefficient at the wavelength of the bleaching band minimum in TA spectrum; ΔOD_S and ΔOD_T are the optical density changes at the minimum of the bleaching band and the maximum of the positive band, respectively. When the ε_T value was obtained, the triplet excited-state quantum yield can be calculated by the relative actinometry,[45] in which SiNc in benzene was used as the reference (ε_{590} = 70 000 M^{-1} cm^{-1}, Φ_T = 0.20).[46]

Nonlinear Transmission Measurement. Using 4.1 ns laser pulses at 532 nm, the nonlinear transmission experiments for Pt complexes were carried out in CH_2Cl_2 solution in a 2-mm cuvette. The linear transmission of the solution was adjusted to 80%. A Quantel Brilliant ns laser with a repetition rate of 10 Hz was used as the light source. The experimental setup and details were described previously.[47] An f = 40 cm plano-convex lens was used to focus the beam to the sample cuvette. The radius of the beam waist at the focal point was approximately 96 μm measured by knife edge.

RESULTS AND DISCUSSION

Electronic Absorption. The UV−vis absorption spectra of the complexes **1** and **2** and ligands **1L** and **2L** in CH_2Cl_2 are presented in Figure 1. The absorption band maxima and molar extinction coefficients are listed in Table 1. The UV−vis absorption of the complexes and ligands obey Beer's law in the concentration range of 1×10^{-6} to 1×10^{-4} mol L^{-1}, suggesting that no dimerization or oligomerization occurs in this concentration range.

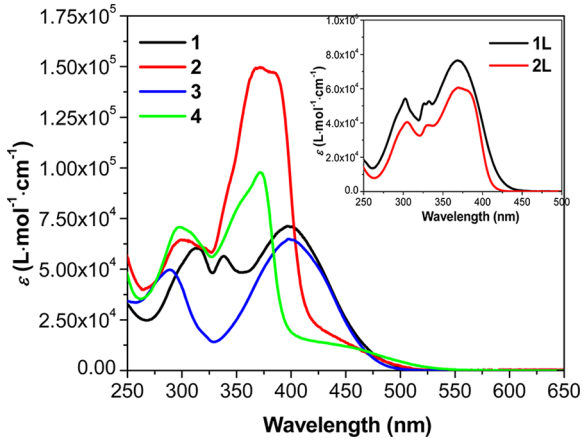

Figure 1. UV−vis absorption spectra of Pt complexes **1**−**4** in CH_2Cl_2. Inset shows the UV−vis absorption spectra of ligands **1L** and **2L** in CH_2Cl_2.

The absorption spectra of **1** and **2** are quite distinct. For complex **1**, the spectrum is dominated by an intense, broad, structureless absorption band at λ_{max} = 397 nm ($\varepsilon \approx 7.1 \times 10^4$ L mol^{-1} cm^{-1}) in CH_2Cl_2. Comparing this absorption band to the corresponding band in ligand **1L**, both bands exhibit similar molar extinction coefficient and similar feature. Therefore, this band should contain significant acetylide ligand based $^1\pi,\pi^*$ character. However, the band in **1** is substantially red-shifted and broadened. On one hand, the red-shift could partially arise from the delocalization of ligand-centered molecular orbital due to the interaction with the Pt(II) dπ orbital. On the other hand, the broadening and red-shift imply admixture of other charge transfer transitions with the $^1\pi,\pi^*$ transition, which is partially reflected by the structureless feature of this band. With reference to the UV−vis absorption spectra of complex **3**[21] and Pt(II) diimine complex with nitrostilbenylacetylide ligands[22] (which all exhibit the similar intense structureless absorption band), this band could be tentatively attributed to acetylide ligand localized $^1\pi,\pi^*$ transition mixed with some ^{1}MLCT/^{1}LLCT transitions. In addition, considering the extended π-conjugation of the acetylide ligands and the strong electron-withdrawing ability of the NO_2 substituent, ^{1}ILCT from the ethynylfluorene component to the nitrophenyl component also likely to contribute to this band. The configurationally mixed transition nature of this absorption band is partially reflected by the minor solvent effect (Figure 2a) and is supported by the TDDFT calculation results that will be discussed later.

The UV−vis absorption spectrum of **2** mainly consists of an intense absorption band at ca. 373 nm and a broad tail from 425 to 525 nm. The similar shape and energy of the 373 nm band to the major absorption band in ligand **2L** suggests that this band should predominantly emanate from the acetylide ligand based $^1\pi,\pi^*$ transitions. The minor solvent effect observed for this band (Figure 2b) supports this assignment. In contrast, the broad tail from 425 to 525 nm displays a negative solvatochromic effect (i.e., the band bathochromically shifts when the polarity of solvent decreases, such as the case in toluene and hexane) (Figures 2b). The negative solvatochromic effect is indicative of a charge-transfer transition in which the dipole moment of the ground state is larger than that of the excited state. Based on the similar results reported for other Pt(II) diimine acetylide complexes[2,4,11,12] and for complex **4**,[21] this band can be attributed to the ^{1}MLCT/^{1}LLCT transitions. This assignment is also supported by the TDDFT calculation results discussed later.

The major absorption bands in **1** and **2** are influenced significantly by the extended π-conjugation in the acetylide ligands. A comparison of **1** and **3** and **2** and **4**, respectively, indicates that the molar extinction coefficients in **1** and **2** are substantially increased; especially in **2** the enhancement is dramatic. In addition, for complex **2**, the ^{1}MLCT/^{1}LLCT band is slightly blue-shifted compared to that in **4**. The blue-shift of the ^{1}MLCT/^{1}LLCT absorption band with increased π-conjugation of the phenylacetylide ligand has also been reported by Che's group[48] and by our group[49] on cyclometalated Pt(II) C∧N∧N complexes.

Calculation of Singlet Excited Electronic States. The ground state equilibrium geometry and the electronic structure of the complexes **1** and **2** were calculated using the B3LYP DFT method in conjunction with LANG631 basis set. All calculations were performed in the condensed phase using the polarizable continuum model (PCM)[38] and CH_2Cl_2 as solvent to maintain close similarity to the experimental conditions. Results of the ground state electronic structure calculations were used to generate the frontier molecular orbital (FMO) electron density plots of four highest occupied molecular orbitals (HOMOs) and four lowest unoccupied molecular

dx.doi.org/10.1021/jp309841x | J. Phys. Chem. A 2013, 117, 1907−1917

Table 1. Photophysical Data for Ligands 1L and 2L and Pt(II) Complexes 1 and 2

	λ_{abs}/nm[a] (ε/10^4 L/mol cm)	λ_{em}/nm (τ_{em}/ns; Φ_{em}) R.T.[b]	λ_{em}/nm (τ_{em}/μs) 77 K[d]	λ_{S1-Sn}/nm (τ_S/ps)[e]	λ_{T1-Tn}/nm (τ_T/ns; ε_{T1-Tn} /10^4 L/mol cm; Φ_T)[f]
1L	303 (5.39), 369 (7.64)	549 (*c*, 0.049)	540 (*c*)	476 (108 ± 2), 552 (sh.,101 ± 2)	478 (1870, 6.51, 0.17)[g]
2L	305 (4.05), 369 (6.07)	448 (*c*, 0.81)	410 (*c*)	555 (sh., 8 ± 1), 651 (17 ± 1)	475 (31200, 3.51, 0.11)[g]
1	314 (6.03), 338 (5.64), 397 (7.13)	576 (25; 0.001)	570 (109), 615 (75)	489 (40 ± 2)	500 (3220, 7.20, 0.15)[h]
2	300 (6.44), 373 (15.0), 450 (1.37)	568 (970; 0.070)	561 (93), 605 (93)	646 (13 ± 1)	550 (610, *i*, *i*)[h]

[a]Electronic absorption band maxima and molar extinction coefficients in CH_2Cl_2 at room temperature. [b]Room temperature emission band maxima and decay lifetimes measured in CH_2Cl_2 at a concentration of 1×10^{-5} mol/L. A degassed aqueous solution of $[Ru(bpy)_3]Cl_2$ (Φ_{em} = 0.042, excited at 436 nm) was used as the reference. [c]Not measured. [d]The emission band maxima and decay lifetimes at 77 K measured in MTHF glassy solution at a concentration of 1×10^{-5} mol/L. [e]fs TA band maxima and singlet excited-state lifetimes in 10:1 (v/v) CH_3CN/CH_2Cl_2 mixture. [f]ns TA band maxima, triplet extinction coefficients, triplet excited-state lifetimes and quantum yields. SiNc in C_6H_6 was used as the reference. (ε_{590} = 70 000 L mol^{-1} cm^{-1}, Φ_T = 0.20). [g]In CH_3CN. [h]In toluene. [i]Too weak to be measured.

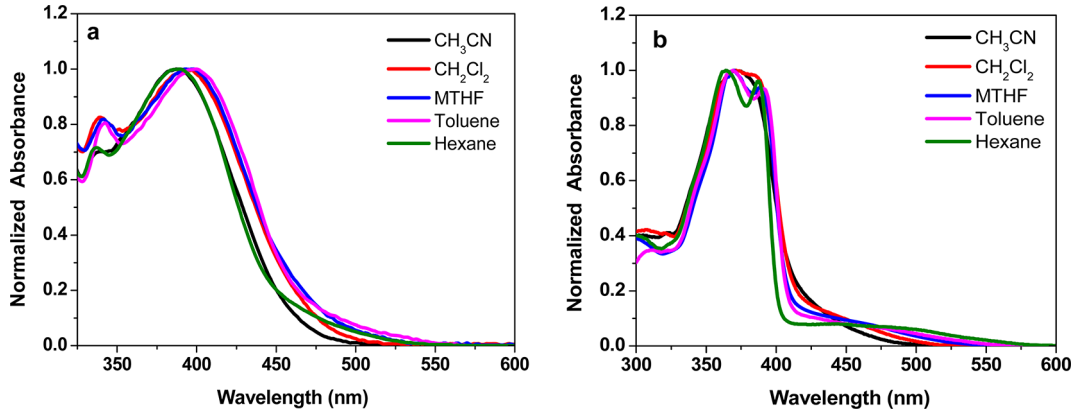

Figure 2. Normalized UV−vis absorption spectra of (a) complex **1** and (b) complex **2** in different solvents. The concentration of each solution was adjusted in order to obtain A = 0.08 at 436 nm in a 1-cm cuvette.

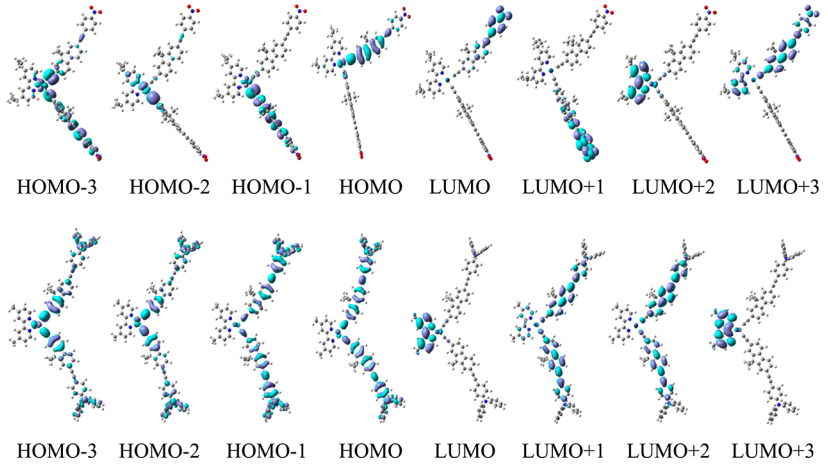

Figure 3. Top: Contour plots of the highest occupied molecular orbital (HOMO), HOMO-1, HOMO-2, HOMO-3, lowest unoccupied molecular orbital (LUMO), LUMO+1, LUMO+2, and LUMO+3 for complex **1**. Bottom: Contour plots of the highest occupied molecular orbital (HOMO), HOMO-1, HOMO-2, and HOMO-3, and lowest unoccupied molecular orbital (LUMO), LUMO+1, LUMO+2, and LUMO+3, for complex **2**.

orbitals (LUMOs) displayed in Figure 3, to assist in the interpretation and assignment of significant electron transitions in the experimentally observed UV−vis absorption spectra.

For complex **1**, the electron density of the HOMO includes contributions from the Pt metal and the ethynylfluorene unit of only one of the acetylide ligands and that of the LUMO is located almost exclusively on the nitrophenylacetylene component of the same acetylide ligand. The HOMO-1 electron density comes from the Pt metal and the other acetylide ligand that does not contribute to the HOMO. Similarly, the electron density of the LUMO+1 is located almost exclusively on the nitrophenylacetylene component of the other acetylide ligand that shows dominant contribution to the HOMO-1 density. For complex **2**, the electron density distributions on the HOMO and HOMO-1 orbitals have similar features; with almost equal contributions from both acetylide ligands and considerable contributions from the Pt metal. The LUMO and LUMO+1 electron densities are quite

dx.doi.org/10.1021/jp309841x | J. Phys. Chem. A 2013, 117, 1907−1917

Table 2. Excitation Energies (eV), Wavelengths (nm), Oscillator Strengths, Main Contributing Transitions, and the Associated Configuration Coefficients of Five Singlet Electronic States of Complexes 1 and 2 Obtained at the CAM-B3LYP/LANG631//B3LYP/LANG631[a] Level of Theory[b]

		excitation energy				
complex	S_n	eV	nm	f	main contributing transitions	configuration coefficients
1	1	3.21	386	2.6303	HOMO → LUMO	0.48
					HOMO → LUMO+3	0.26
	2	3.30	375	1.8968	HOMO-1 → LUMO+1	0.53
	3	3.49	355	0.1099	HOMO → LUMO+2	0.55
	4	3.61	343	0.0001	HOMO-1 → LUMO+2	0.59
	5	3.85	322	0.1609	HOMO-2 → LUMO+2	0.56
2	1	3.22	384	1.9284	HOMO → LUMO	0.42
					HOMO-2 → LUMO	0.38
	2	3.34	370	1.3008	HOMO-3 → LUMO	0.37
					HOMO-1 → LUMO	0.34
	3	3.48	356	2.5675	HOMO → LUMO+1	0.40
					HOMO-1 → LUMO+2	0.37
	4	3.57	346	0.2158	HOMO → LUMO+2	0.35
					HOMO-1 → LUMO+1	0.35
					HOMO-3 → LUMO	0.32
	5	3.88	319	0.0091	HOMO-5 → LUMO	0.48
					HOMO-4 → LUMO	0.36
					HOMO-6 → LUMO	0.30

[a]LANG631 basis set refers to 6-31G* for C, H, N, and S and LANL2DZ for Pt. [b]All calculation results are corrected for solvent effects using the PCM model.

different; the dominant contribution to the LUMO is almost exclusively from the π^*(bipyridine) component, while the LUMO+1 orbital shows dominant contributions from the phenylethynylfluorenylacetylene components of the two acetylide ligands.

Theoretical UV−vis absorption spectra were calculated at the CAM-B3LYP/LANG631//B3LYP/LANG631 model chemistry; with the inclusion of solvent correction effects using the PCM model and CH_2Cl_2 as solvent. The excitation energies (eV), wavelengths (nm), oscillator strengths, dominant contributing transitions, and the associated configuration coefficients of several singlet excited electronic states of complexes **1** and **2** are presented in Table 2. Results of the TDDFT calculations for complex **1** indicate that the lowest energy absorption band involves two main electronic transitions: HOMO → LUMO and HOMO → LUMO+3, which correspond to the first excited state with excitation wavelength of 386 nm. The second lowest energy absorption band maximum (2nd excited state) occurs at 375 nm and involves the HOMO-1 → LUMO+1 electron transition. For complex **2**, three significant low-lying electronic transitions were obtained from the calculations: HOMO → LUMO and HOMO-2 → LUMO (1st excited state, occurred at 384 nm), HOMO-3 → LUMO and HOMO-1 → LUMO (2nd excited state, occurred at 370 nm), and HOMO → LUMO+1 and HOMO-1 → LUMO+2 (3rd excited state, occurred at 356 nm). The calculated excitation wavelengths for these complexes are in semiquantitative agreement with the experimentally measured λ_{max} shown in Table 1; which can be expected considering that the complexes are large and, thus, limit the use of larger basis sets that can improve the predicted excitation energies. The results obtained for these complexes for the first three excited states show an absolute deviation from experiment of 11−41 nm for complex **1** and 3−66 nm for complex **2**. These are actually nice results for such large molecules and indicate that the CAM-B3LYP functional is a good performer for predicting excited state energies of molecules involving charge transfer transitions as has been observed in other organic dye systems.[50]

Based on the electron density distribution on the FMOs and the predicted vertical excitation energies, the lowest-energy absorption bands for these complexes should arise from ^{1}LLCT/^{1}ILCT/^{1}MLCT/$^1\pi,\pi^*$ transitions for **1**, and the ^{1}LLCT/^{1}MLCT transitions for **2**. This is consistent with the experimental data of the ground-state absorption, and further supports the absorption band assignments. It is worth noting that for complex **1**, the ^{1}ILCT and acetylide ligand-based $^1\pi,\pi^*$ transitions (HOMO → LUMO+3) partially overlap with the ^{1}LLCT/^{1}MLCT transition bands and the charge transfer band observed from the UV−vis measurement is an intense, structureless absorption band. Additionally, because the FMOs are localized only on one of the acetylide ligands in **1**, the molar extinction coefficient for the major absorption band in **1** is much smaller than that for the major absorption band in **2**, in which the HOMOs are delocalized on both acetylide ligands.

Emission. The steady-state emission spectra of complexes **1** and **2** were measured in different solvents at R.T. and in butyronitrile matrix at 77 K. The normalized emission spectra of the Pt complexes and their respective acetylide ligands in CH_2Cl_2 are illustrated in Figure 4. The fluorescence spectra of **L1** and **L2** exhibit structureless feature and positive solvatochromic effect (Supporting Information, Figure S3 and S4), indicating an intramolecular charge-transfer (ICT) emission. In contrast, excitation of **1** and **2** in CH_2Cl_2 solution at their respective charge-transfer band produces orange luminescence, which can be quenched by oxygen. Their emission spectra exhibit significant Stokes shifts, relatively sharp and narrow shape, with emission lifetimes of 25 ns for **1** and approximately 1 μs for **2** in deaerated CH_2Cl_2. Taking into account these pieces of information, we believe that their emission emanates from the first triplet excited state (T_1).

dx.doi.org/10.1021/jp309841x | J. Phys. Chem. A 2013, 117, 1907−1917

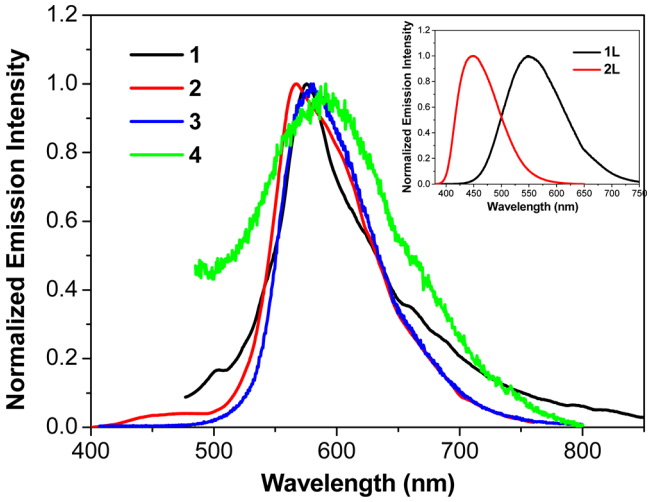

Figure 4. Normalized emission spectra of Pt complexes **1** (λ_{ex} = 463 nm), **2** (λ_{ex} = 450 nm), **3** (λ_{ex} = 397 nm), and **4** (λ_{ex} = 475 nm) in CH_2Cl_2 ($c = 1 \times 10^{-5}$ mol L^{-1}). Inset shows the normalized emission spectra of ligand **1L** (λ_{ex} = 379 nm) and **2L** (λ_{ex} = 370 nm) in CH_2Cl_2.

However, the nature of the emitting state of **1** and **2** varies in different solvents. The emission energies, lifetimes and quantum yields in different solvents are summarized in Table 3. As shown in Figure 5a for complex **1**, a minor solvatochromic effect was observed. The emission was significantly quenched in polar solvents, such as CH_3CN and CH_2Cl_2. In contrast, in low-polarity solvents like toluene and hexane, the lifetime becomes much longer compared to those in polar solvents, which is indicative of a charge-transfer emitting state in polar solvents. However, compared to **3**,[21] the emission spectrum of **1** is more structured and relatively narrower; and the emission lifetime is also significantly longer. Considering that the emission of complex **3** was attributed to a triplet charge transfer (CT) state caused by the strong electron-withdrawing NO_2 substituent,[21] and the extended π-conjugation could significantly admix the $^3\pi,\pi^*$ character into the lowest triplet excited state, we attribute the emitting state of **1** to mixed ^{3}CT/$^3\pi,\pi^*$ states (where the charge transfer states could be ^{3}MLCT/^{3}LLCT/^{3}ILCT). In the case of complex **2** (shown in Figure 5b and Table 3), a structured emission band in CH_2Cl_2 (vibronic spacing of ~1159 cm^{-1}) with a longer emission lifetime (~1 μs in CH_2Cl_2) was observed. This indicates that the emitting state in polar solvent could be dominated by the $^3\pi,\pi^*$ excited state that is mainly localized on the acetylide ligands, possibly mixed with some ^{3}MLCT/^{3}LLCT characters. On the contrary, the negative solvatochromic effect, structureless feature, and shorter lifetime in low-polarity solvents imply that the emitting state is predominantly ^{3}MLCT/^{3}LLCT in low-polarity solvents. Similar solvent-induced switch between the $^3\pi,\pi^*$ dominated emission and ^{3}MLCT/^{3}LLCT dominated emission in other Pt(II) diimine complexes has also been reported previously by Castellano's group[11] and our group.[15] It is noted that complex **4** only shows a very weak emission band in CH_2Cl_2, which was ascribed to the enhanced ICT (intramolecular charge transfer) state, particularly the ^{3}LLCT state caused by the electron-donating NPh_2 group.[21] With the extension of π-conjugation in the acetylide ligands, the nature of emitting state could be altered by admixing $^3\pi,\pi^*$ character with the ^{3}MLCT/^{3}LLCT excited states in **2**. This configurational mixing is probably accounted for the blue-shift of the emission band in **2** compared to that in **4**. The blue-shift of the emission band with extended π-conjugation in the acetylide ligand has also been observed in Pt(II) C^N^N complexes by Che and co-workers previously.[48]

The emission of **1** and **2** in BuCN glassy matrix at 77 K was investigated to better understand the nature of their emissive triplet excited states. As shown in Figure 5, their emission spectra at 77 K are blue-shifted and become narrower and more structured. The lifetimes are also much longer compared to those at room temperature. The thermally induced Stokes shift (ΔE_s) is relatively small for both complexes (~ 554 cm^{-1} for **1** and ~933 cm^{-1} for **2**). The small ΔE_s values indicate that the triplet emitting states of **1** and **2** indeed possess substantial $^3\pi,\pi^*$ characters.

Transient Absorption. The fs (Figure 6) and ns (Figure 7) TA spectra of complexes **1** and **2** were investigated to further understand the properties of both singlet and triplet excited states. The time-resolved fs TA spectra of **1** and **2** in CH_3CN/CH_2Cl_2 are presented in Figure 6a,b, and the singlet excited-state lifetimes deduced from the fs TA decay profiles are listed in Table 1. The fs TA spectroscopic study not only provides the singlet excited-state difference absorption spectrum, but also deduces the singlet excited state lifetime that cannot be obtained from the decay of fluorescence due to the undetectable fluorescence in many Pt(II) complexes.

As illustrated in Figure 6, complexes **1** and **2** both exhibit positive absorption bands from 450 to 800 nm, which resemble the spectral region of their respective ligands (Supporting Information, Figures S5 and S6) but with somewhat different shapes. This indicates that their singlet excited state absorptions should partially originate from the ^{1}ILCT/$^1\pi,\pi^*$ excited states of the acetylide ligands. Immediately following the 400 nm excitation, ultrafast intersystem crossing occurs for complexes **1** and **2**. The shapes of the TA spectra of complex **1** remain the same over the whole time range of the ~1.4 ns delay line after the 400-nm excitation, which are quite similar to those measured by ns laser flash photolysis (Figure 6d). The minor difference between the fs TA and ns TA spectra could be due to the different solvents used in these two measurements. For complex **2**, the intensity of the fs TA spectrum decreases within 1.7 ps after excitation; then the intensity of the spectrum increases to the maximum at 23 ps delay and then decay relatively slowly. This feature implies a fast intersystem crossing in less than 23 ps from the singlet to the triplet excited state

Table 3. Emission Energies, Lifetimes and Quantum Yields of Complexes 1 and 2 in Different Solvents at R.T.

	λ_{em}/nm (τ_{em}/ns; Φ_{em})[a]				
	CH_3CN	CH_2Cl_2	MTHF	toluene	hexane
1	*b*	576 (25; 0.001)	595 (190; 0.005)	581 (1330; 0.061)	578 (2790; 0.071)
2	*b*	568 (970; 0.070)	592 (225; 0.046)	594 (365; 0.12)	597 (440; 0.14)

[a]The spectra and lifetimes were measured in dilute solutions with an absorbance of approximately 0.08 at 436 nm in a 1-cm cuvette. A degassed aqueous solution of $[Ru(bpy)_3]Cl_2$ (Φ_{em} = 0.042, excited at 436 nm) was used as the reference. [b]Too weak to be measured.

dx.doi.org/10.1021/jp309841x | J. Phys. Chem. A 2013, 117, 1907−1917

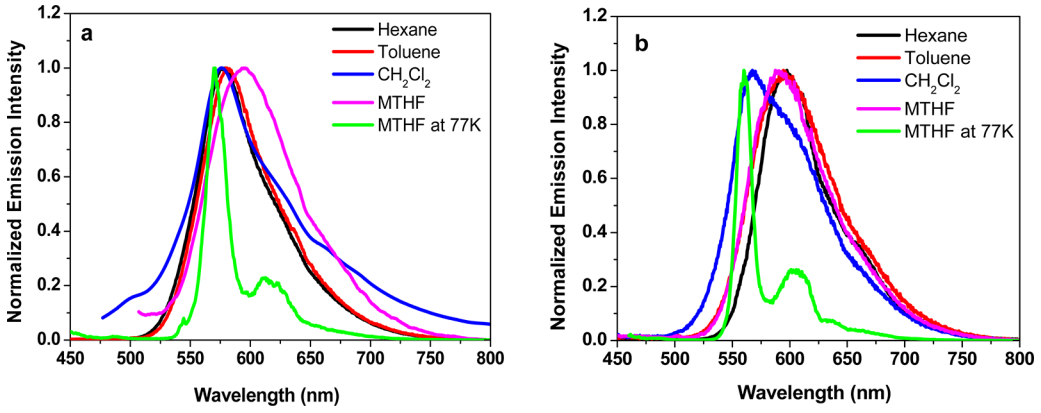

Figure 5. Normalized emission spectra of (a) complex **1** and (b) complex **2** in different solvents at room temperature and in BuCN glassy matrix at 77 K, λ_{ex} = 436 nm.

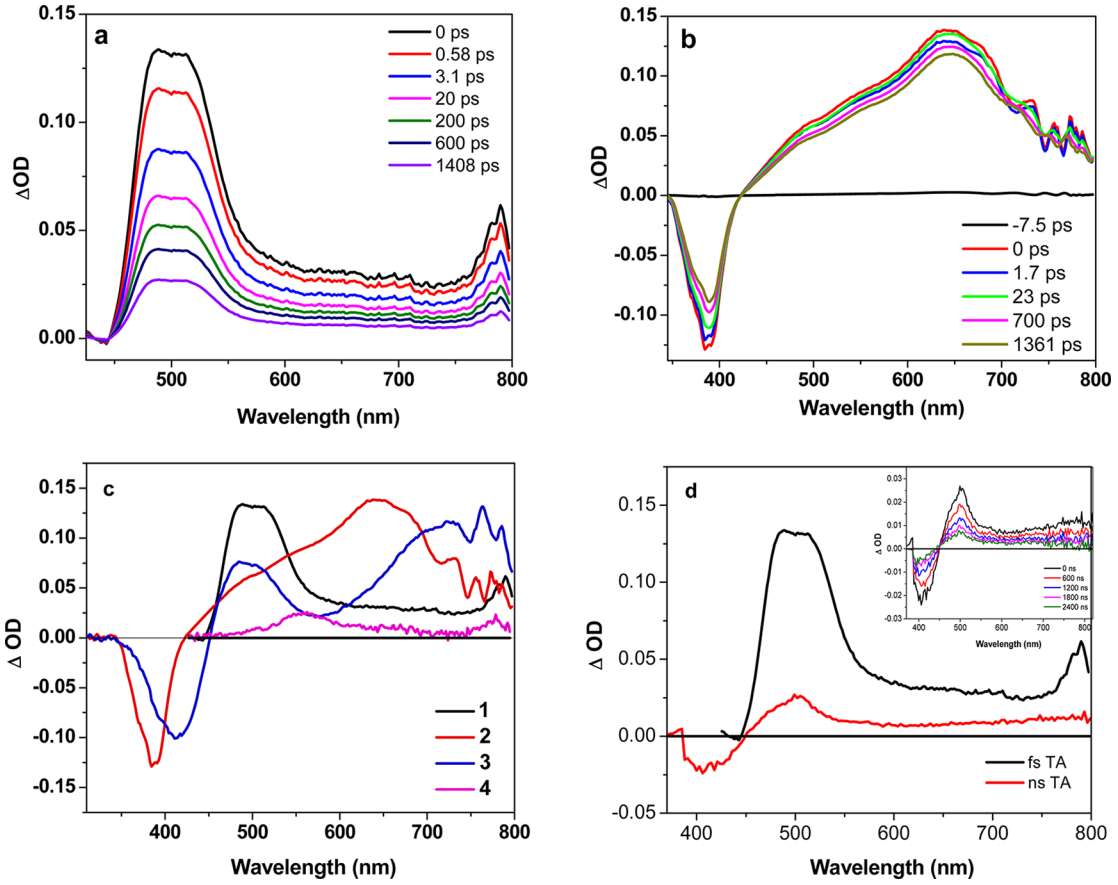

Figure 6. (a) Time-resolved fs TA spectrum of complex **1** in 10:1 (v/v) CH_3CN/CH_2Cl_2; (b) Time-resolved fs TA spectrum of complex **2** in 12:1 (v/v) CH_3CN/CH_2Cl_2; (c) Comparison of the fs TA spectra of complexes **1**–**4** in CH_3CN/CH_2Cl_2 mixture (**1**, 10:1; **2**, 12:1; **3**, 12:1; **4**, 1:1) at zero delay after excitation; (d) Comparison of the fs and ns TA spectra of **1** at zero delay after excitation. λ_{ex} = 400 nm for fs TA and λ_{ex} = 355 nm for ns TA measurements. The fs TA spectrum was measured in mixed 10:1 (v/v) CH_3CN/CH_2Cl_2 solution; while the ns TA spectrum was measured in toluene solution with A_{355} = 0.4 in a 1-cm cuvette. The inset shows the time-resolved ns TA spectrum of **1** in toluene.

and the triplet excited state exhibits a very similar absorption spectrum to that of the singlet excited state. Kinetic study of the triplet excited-state absorption at 550 nm reveals that the decay of the absorbing triplet excited state is approximately 610 ns. Unfortunately, the full ns TA spectrum of **2** was unable to be measured due to the very weak signal under our ns TA experimental condition. However, the fs TA spectra at longer decay times (>23 ps) indicate that the triplet excited state of **2** absorbs broadly from 430 to 800 nm. For complex **1**, both fs TA and ns TA spectral features resemble the ns TA spectrum of **1L** (Supporting Information, Figure S7) and the fs TA spectrum of **1L** at longer delay (Supporting Information, Figure S5). Considering this character and the much longer lifetime (τ_T = 3.2 μs), the excited states that contribute to the observed fs and ns TA for complex **1** should be dominated by the $^1\pi,\pi^*/^1$ILCT and $^3\pi,\pi^*/^3$ILCT states, respectively, possibly mixed with some MLCT/LLCT characters. For complex **2**, considering the nature of the lowest singlet excited state being

dx.doi.org/10.1021/jp309841x | J. Phys. Chem. A 2013, 117, 1907–1917

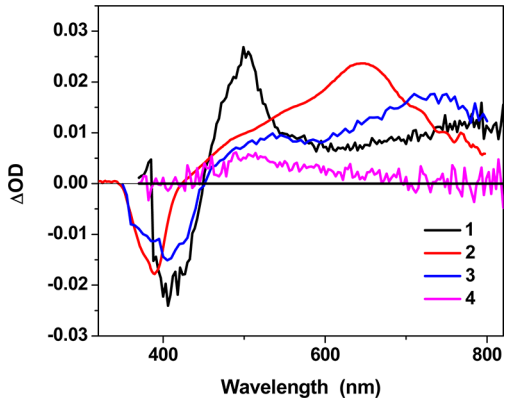

Figure 7. Comparison of the triplet transient difference absorption spectra of **1**−**4**. Complexes **1** and **3** were measured in toluene, and **4** was measured in 9:1 (v/v) toluene/CH_2Cl_2 with A_{355} = 0.4 in a 1-cm cuvette, λ_{ex} = 355 nm, the delay time was zero. The spectrum of complex **2** was measured by fs TA in 12:1 (v/v) CH_3CN/CH_2Cl_2 at a time delay of 1361 ps after excitation, λ_{ex} = 400 nm. The spectrum of **2** was scaled to 1/5 of the original intensity for comparison purpose.

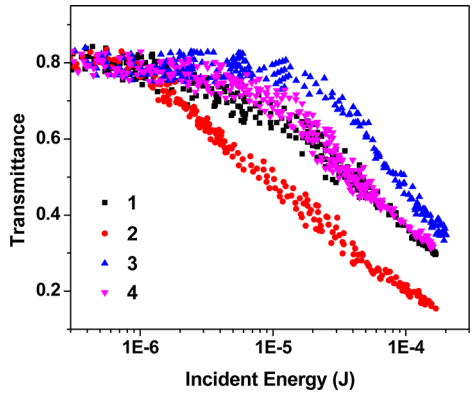

Figure 8. Nonlinear transmission curves for Pt complexes **1**−**4** in CH_2Cl_2 for 4.1 ns laser pulses at 532 nm. The linear transmission for all samples was adjusted to 80% in a 2-mm cuvette.

^{1}MLCT/^{1}LLCT as discussed earlier and the similar spectral region to its corresponding ligand, the observed fs TA is presumably attributed to ^{1}MLCT/^{1}LLCT probably mixed with some $^1\pi,\pi^*/^1$ILCT characters.

It is worth noting that the fs TA spectra of **1** and **3** (Figure 6c) are similar in that both of them possess a strong absorption band in the visible and another band in the NIR spectral region. However, the NIR band in **3** is much broader and stronger than that in **1** although the NIR band in **1** is red-shifted. In contrast, the fs TA spectrum of **2** at zero delay is pronouncedly broadened and red-shifted compared to that of **4**. The same trend is observed for the triplet transient absorption spectra of **1** and **3**, and **2** and **4** (Figure 7). The different features in the respective fs and ns TA spectra of **1** and **3**, and **2** and **4** reflect the influence of the extended π-conjugation of the acetylide ligand on the singlet and triplet excited-state absorption. Meanwhile, the observed trend implies that the transient absorbing species in **2** should be closely related to the acetylide ligand, which could possibly be the LLCT, π,π^*, or ILCT states.

Reverse Saturable Absorption. Our TA study indicates that complexes **1** and **2** exhibit stronger excited-state absorption than ground-state absorption in the visible to near-IR spectral region. Thus, reverse saturable absorption (RSA, i.e., transmission of sample solution decreases with increased incident energy) is anticipated to occur in this spectral region. To demonstrate this, the transmission vs incident energy experiment at 532 nm was carried out in a 2-mm cuvette in CH_2Cl_2 solutions using 4.1 ns laser pulses, and the results are shown in Figure 8. For easy comparison, the concentrations of **1** and **2** were adjusted in order to obtain a linear transmission of 80% at 532 nm. To manifest the effect of extended π-conjugation of the acetylide ligand on the RSA, the nonlinear transmission curves of **3** and **4** at the identical experimental conditions are provided in Figure 8 as well. Obviously, with increased incident energy, the transmission of **1**−**4** all decrease drastically, which clearly indicates the occurrence of RSA at 532 nm. Compared to **3** and **4**, the strength of the RSA at 532 nm for complexes **1** and **2** is significantly increased. For example, complex **4** shows a RSA threshold (defined as the incident energy at 70% of the linear transmittance) of 26.1 μJ and the transmission decreases to 0.31 when the incident energy reaches ∼170 μJ. In contrast, for complex **2**, its RSA threshold decreases to 5.1 μJ and the transmission decreases to 0.15 when the incident energy reaches ∼170 μJ. The respective 5- and 2-fold decreases in the RSA threshold and transmission suggests that extension of π-conjugation of the acetylide ligand dramatically increases the degree of RSA in the studied complexes; and, hence, demonstrating that RSA in Pt(II) diimine complexes can be improved by extending the π-conjugation of the acetylide ligands. This provides a useful approach for developing efficient nonlinear absorbing materials.

CONCLUSION

Two new Pt(II) diimine bis(phenylethynylfluorenylacetylide) complexes with terminal NO_2 and NPh_2 substituents (**1** and **2**) were synthesized and their photophysical properties were systematically investigated. Complex **1** exhibits intense structureless absorption at ∼397 nm, which is attributed to the $^1\pi,\pi^*/^1$ILCT/^{1}LLCT/^{1}MLCT transitions. Complex **2** possesses a very intense acetylide ligands localized $^1\pi,\pi^*$ absorption band at ∼373 nm and broad ^{1}MLCT/^{1}LLCT transition tail from 425 to 525 nm. The ground state electronic structure and vertical excitation energies of several excited singlet electronic states were computed using DFT (B3LYP) and TDDFT (CAM-B3LYP) methods, respectively, and the results of the calculations assisted in the interpretation and assignment of the UV−vis absorption bands. The emitting state of **1** was found to be mixed ^{3}CT/$^3\pi,\pi^*$ states; while the emitting state of **2** exhibits a switch from predominantly $^3\pi,\pi^*$ state in high-polarity solvents to ^{3}MLCT/^{3}LLCT states in low-polarity solvents. The fs TA study indicates that **1** and **2** exhibit ultrafast intersystem crossing and broadband excited-state absoprtion in 450−800 nm. Their triplet excited states appear to be populated via rapid intersystem crossing in only a few picoseconds after laser excitation. In addition, strong RSA was observed at 532 nm for ns laser pulses from **1** and **2**, which are drastically stronger than each of their corresponding complex with shorter π-conjugation in their acetylide ligands, i.e., **3** and **4**, respectively. The photophysical and nonlinear transmission studies revealed that extending the π-conjugation of the acetylide ligand can alter the singlet and triplet excited state properties substantially and improve the RSA at 532 nm drastically. The broad excited-state absorption and strong nonlinear transmittance performance at 532 nm for **1** and **2** suggest that these complexes could be promising candidates as broadband nonlinear absorbing materials.

dx.doi.org/10.1021/jp309841x | J. Phys. Chem. A 2013, 117, 1907−1917

■ ASSOCIATED CONTENT

Supporting Information

Solvent-dependency UV−vis and emission spectra of **1L** and **2L**, time-resolved fs and ns transient difference absorption spectra of **1L** and **2L**, TDDFT calculation results for **1** and **2**, and the full author list for ref 39. This material is available free of charge via the Internet at http://pubs.acs.org.

■ AUTHOR INFORMATION

Corresponding Author

*E-mail: Wenfang.Sun@ndsu.edu. Phone: 701-231-6254. Fax: 701-231-8831.

Notes

The authors declare no competing financial interest.

■ ACKNOWLEDGMENTS

This work is partially supported by the National Science Foundation (CAREER CHE-0449598) and partially supported by the Army Research Laboratory (W911NF-10-2-0055).

■ REFERENCES

(1) Williams, J. A. G. Photochemistry and Photophysics of Coordination Compounds: Platinum. *Top. Curr. Chem.* **2007**, *281*, 205−268.

(2) Hissler, M.; McGarrah, J. E.; Connick, W. B.; Geiger, D. K.; Cummings, S. D.; Eisenberg, R. Platinum Diimine Complexes: Towards a Molecular Photochemical Device. *Coord. Chem. Rev.* **2000**, *208*, 115−137.

(3) McGarrah, J. E.; Kim, Y.-J.; Hissler, M.; Eisenberg, R. Toward a Molecular Photochemical Device: A Triad for Photoinduced Charge Separation Based on a Platinum Diimine Bis(acetylide) Chromophore. *Inorg. Chem.* **2001**, *40*, 4510−4511.

(4) Suzuki, S.; Sugimura, R.; Kozaki, M.; Keyaki, K.; Nozaki, K.; Ikeda, N.; Akiyama, K.; Okada, K. Highly Efficient Photoproduction of Charge-Separated States in Donor-Acceptor-Linked Bis(acetylide) Platinum Complexes. *J. Am. Chem. Soc.* **2009**, *131*, 10374−10375.

(5) Liu, Y.; Li, Q.; Zhao, J.; Guo, H. BF_2-bound Chromophore-containing N̂N Pt(II) Bisacetylide Complex and Its Application as Sensitizer for Triplet−triplet Annihilation Based Upconversion. *R. Soc. Chem. Adv.* **2012**, *2*, 1061−1067.

(6) Liu, Y.; Wu, W.; Zhao, J.; Zhang, X.; Guo, H. Accessing the Long-lived Near-IR-emissive Triplet Excited State in Naphthalenediimide with Light-harvesting Diimine Platinum(II) Bisacetylide Complex and Its Application for Upconversion. *Dalton Trans.* **2011**, *40*, 9085−9089.

(7) Huang, L.; Zeng, L.; Guo, H.; Wu, W.; Wu, W.; Ji, S.; Zhao, J. Room-Temperature Long-Lived ^{3}IL Excited State of Rhodamine in an *N̂N* Pt^{II} Bis(acetylide) Complex with Intense Visible-Light Absorption. *Eur. J. Inorg. Chem.* **2011**, 4527−4533.

(8) Sun, H.; Guo, H.; Wu, W.; Liu, X.; Zhao, J. Coumarin Phosphorescence Observed with *N̂N* Pt(II) Bisacetylide Complex and Its Applications for Luminescent Oxygen Sensing and Triplet−triplet-annihilation Based Upconversion. *Dalton Trans.* **2011**, *40*, 7834−7841.

(9) Li, Q.; Guo, H.; Ma, L.; Wu, W.; Liu, Y.; Zhao, J. Tuning the Photophysical Properties of N̂N Pt(II) Bisacetylide Complexes with Fluorene Moiety and Its Applications for Triplet−triplet-annihilation Based Upconversion. *J. Mater. Chem.* **2012**, *22*, 5319−5329.

(10) Chan, S.-C.; Chan, M. C. W.; Wang, Y.; Che, C.-M.; Cheung, K.-K.; Zhu, N. Organic Light-Emitting Materials Based on Bis(arylacetylide)platinum(II) Complexes Bearing Substituted Bipyridine and Phenanthroline Ligands: Photo- and Electroluminescence from ^{3}MLCT Excited States. *Chem.—Eur. J.* **2001**, *7*, 4180−4190.

(11) Pomestchenko, I. E.; Castellano, F. N. Solvent Switching between Charge Transfer and Intraligand Excited States in a Multichromophoric Platinum(II) Complex. *J. Phys. Chem. A* **2004**, *108*, 3485−3492.

(12) Pomestchenko, I. E.; Luman, C. R.; Hissler, M.; Ziessel, R.; Castellano, F. N. Room Temperature Phosphorescence from a Platinum(II) Diimine Bis(pyrenylacetylide) Complex. *Inorg. Chem.* **2003**, *42*, 1394−1396.

(13) Guo, H.; Ji, S.; Wu, W.; Wu, W.; Shao, J.; Zhao, J. Long-lived Emissive Intra-ligand Triplet Excited States (^{3}IL): Next Generation Luminescent Oxygen Sensing Scheme and a Case Study with Red Phosphorescent Diimine Pt(II) Bis(acetylide) Complexes Containing Ethynylated Naphthalimide or Pyrene Subunits. *Analyst* **2010**, *135*, 2832−2840.

(14) Guo, H.; Muro-Small, M. L.; Ji, S.; Zhao, J.; Castellano, F. N. Naphthalimide Phosphorescence Finally Exposed in a Platinum(II) Diimine Complex. *Inorg. Chem.* **2010**, *49*, 6802−6804.

(15) Sun, W.; Zhang, B.; Li, Y.; Pritchett, T. M.; Li, Z.; Haley, J. E. Broadband Nonlinear Absorbing Platinum 2,2′-Bipyridine Complex Bearing 2-(Benzothiazol-2′-yl)-9,9-diethyl-7-ethynylfluorene Ligands. *Chem. Mater.* **2010**, *22*, 6384−6392.

(16) Pritchett, T. M.; Sun, W.; Zhang, B.; Ferry, M. J.; Li, Y.; Haley, J. E.; Mackie, D. M.; Shensky, W., III; Mott, A. G. Excited-state absorption of a bipyridyl platinum(II) complex with alkynyl-benzothiazolylfluorene units. *Opt. Lett.* **2010**, *35*, 1305−1307.

(17) Zhang, B.; Li, Y.; Liu, R.; Pritchett, T. M.; Azenkeng, A.; Ugrinov, A.; Haley, J. E.; Li, Z.; Hoffmann, M. R.; Sun, W. Synthesis, Structural Characterization, Photophysics, and Broadband Nonlinear Absorption of a Platinum(II) Complex with the 6-(7-Benzothiazol-2′-yl-9,9-diethyl-9*H*-fluoren-2-yl)-2,2′-bipyridinyl Ligand. *Chem.—Eur. J.* **2012**, *18*, 4593−4606.

(18) Wadas, T. J.; Lachicotte, R. J.; Eisenberg, R. Synthesis and Characterization of Platinum Diimine Bis(acetylide) Complexes Containing Easily Derivatizable Aryl Acetylide Ligands. *Inorg. Chem.* **2003**, *42*, 3772−3778.

(19) Hissler, M.; Connick, W. B.; Geiger, D. K.; McGarrah, J. E.; Lipa, D.; Lachicotte, R. J.; Eisenberg, R. Platinum Diimine Bis(acetylide) Complexes: Synthesis, Characterization, and Luminescence Properties. *Inorg. Chem.* **2000**, *39*, 447−457.

(20) Whittle, C. E.; Weinstein, J. A.; George, M. W.; Schanze, K. S. Photophysics of Diimine Platinum(II) Bis-Acetylide Complexes. *Inorg. Chem.* **2001**, *40*, 4053−4062.

(21) Liu, R.; Zhou, D.; Azenkeng, A.; Li, Z.; Li, Y.; Glusac, K. D.; Sun, W. Nonlinear Absorbing Platinum(II) Diimine Complexeses: Synthesis, Photophysics, and Reverse Saturable Absorption. *Chem.—Eur. J.* **2012**, *18*, 11440−11448.

(22) Li, Z.; Badaeva, E.; Zhou, D.; Bjorgaard, J.; Glusac, K. D.; Killina, S.; Sun, W. Tuning Photophysics and Nonlinear Absorption of Bipyridyl Platinum(II) Bisstilbenylacetylide Complexes by Auxiliary Substituents. *J. Phys. Chem. A* **2012**, *116*, 4878−4889.

(23) She, C.; Rachford, A. A.; Wang, X.; Goeb, S.; El-Ballouli, A. A. O.; Castellano, F. N.; Hupp, J. T. Solvent-induced Configuration Mixing and Triplet Excited-state Inversion: Insights from Transient Absorption and Transient dc Photoconductivity Measurements. *Phys. Chem. Chem. Phys.* **2009**, *11*, 8586−8591.

(24) Goeb, S.; Rachford, A. A.; Castellano, F. N. Solvent-induced Configuration Mixing and Triplet Excited State Inversion Exemplified in a Pt(II) Complex. *Chem. Commun.* **2008**, 814−816.

(25) Liu, R.; Azenkeng, A.; Li, Y.; Sun, W. Long-lived Platinum(II) Diimine Complexes with Broadband Excited-state Absorption: Efficient Nonlinear Absorbing Materials. *Dalton Trans.* **2012**, *41*, 12353−12357.

(26) Haley, J. E.; Krein, D. M.; Monahan, J. L.; Burke, A. R.; McLean, D. G.; Slagle, J. E.; Fratini, A.; Cooper, T. M. Photophysical Properties of a Series of Electron-Donating and -Withdrawing Platinum Acetylide Two-Photon Chromophores. *J. Phys. Chem. A* **2011**, *115*, 265−273.

(27) Becke, A. D. Density-functional Thermochemistry. III. The Role of Exact Exchange. *J. Chem. Phys.* **1993**, *98*, 5648−5652.

(28) Lee, C.; Yang, W.; Parr, R. G. Development of the Colle-Salvetti Correlation-energy Formula into a Functional of the Electron Density. *Phys. Rev. B* **1988**, *37*, 785−789.

(29) Yanai, T.; Tew, D. P.; Handy, N. C. A New Hybrid Exchange–correlation Functional Using the Coulomb-attenuating Method (CAM-B3LYP). *Chem. Phys. Lett.* **2004**, *393*, 51–57.
(30) Clark, T.; Chandrasekhar, J.; Spitznagel, G. W.; Schleyer, P. V. R. Efficient Diffuse Function-augmented Basis Sets for Anion Calculations. III. The 3-21+G Basis Set for First-row Elements, Li–F. *J. Comput. Chem.* **1983**, *4*, 294–301.
(31) Francl, M. M.; Pietro, W. J.; Hehre, W. J.; Binkley, J. S.; Gordon, M. S.; DeFrees, D. J.; Pople, J. A. Self-consistent Molecular Orbital Methods. XXIII. A Polarization-type Basis Set for Second-row Elements. *J. Chem. Phys.* **1982**, *77*, 3654–3665.
(32) Gill, P. M. W.; Johnson, B. G.; Pople, J. A.; Frisch, M. J. The Performance of the Becke-Lee-Yang-Parr (B-LYP) Density Functional Theory with Various Basis Sets. *Chem. Phys. Lett.* **1992**, *197*, 499–505.
(33) Hariharan, P. C.; Pople, J. A. Influence of Polarization Functions on MO Hydrogenation Energies. *Theor. Chim. Acta* **1973**, *28*, 213–222.
(34) Krishnan, R.; Binkley, J. S.; Seeger, R.; Pople, J. A. Self-consistent Molecular Orbital Methods. XX. A Basis Set for Correlated Wave Functions. *J. Chem. Phys.* **1980**, *72*, 650–654.
(35) Hay, P. J.; Wadt, W. R. Ab Initio Effective Core Potentials for Molecular Calculations. Potentials for K to Au Including the Outermost Core Orbitals. *J. Chem. Phys.* **1985**, *82*, 299–310.
(36) Hay, P. J.; Wadt, W. R. Ab Initio Effective Core Potentials for Molecular Calculations. Potentials for the Transition Metal Atoms Sc to Hg. *J. Chem. Phys.* **1985**, *82*, 270–283.
(37) Wadt, W. R.; Hay, P. J. Ab Initio Effective Core Potentials for Molecular Calculations. Potentials for Main Group Elements Na to Bi. *J. Chem. Phys.* **1985**, *82*, 284–298.
(38) Tomasi, J.; Mennucci, B.; Cammi, R. Quantum Mechanical Continuum Solvation Models. *Chem. Rev.* **2005**, *105*, 2999–3094.
(39) Frisch, M. J. T.; G., W.; Schlegel, H. B.; Scuseria, G. E.; Robb, M. A.; Cheeseman, J. R.; Scalmani, G.; Barone, V.; Mennucci, B.; Petersson, G. A. et al. *Gaussian 09*, revision A.1; Gaussian, Inc.: Wallingford, CT, 2009.
(40) Demas, J. N.; Crosby, G. A. The Measurement of Photoluminescence Quantum Yields. A Review. *J. Phys. Chem.* **1971**, *75*, 991–1024.
(41) Van Houten, J.; Watts, R. J. Temperature Dependence of the Photophysical and Photochemical Properties of the Tris(2,2′-bipyridyl)ruthenium(II) Ion in Aqueous Solution. *J. Am. Chem. Soc.* **1976**, *98*, 4853–4858.
(42) Melhuish, W. H. Quantum Efficiencies of Fluorescence of Organic Substances: Effect of Solvent and Concentration of the Fluorescent Solute. *J. Phys. Chem.* **1961**, *65*, 229–235.
(43) Zhou, D.; Mirzakulova, E.; Khatmullin, R.; Schapiro, I.; Olivucci, M.; Glusac, K. D. Fast Excited-State Deactivation in N(5)-Ethyl-4a-hydroxyflavin Pseudobase. *J. Phys. Chem. B* **2011**, *115*, 7136–7143.
(44) Carmichael, I.; Hug, G. L. Triplet–Triplet Absorption Spectra of Organic Molecules in Condensed Phases. *J. Phys. Chem. Ref. Data* **1986**, *15*, 1–250.
(45) Kumar, C. V.; Qin, L.; Das, P. K. Aromatic Thioketone Triplets and Their Quenching Behaviour Towards Oxygen and Di-t-butylnitroxy Radical. A Laser-flash-photolysis Study. *J. Chem. Soc., Faraday Trans.* **1984**, *80*, 783–793.
(46) Firey, P. A.; Ford, W. E.; Sounik, J. R.; Kenney, M. E.; Rodgers, M. A. Silicon Naphthalocyanine Triplet State and Oxygen: A Reversible Energy-Transfer Reaction. *J. Am. Chem. Soc.* **1988**, *110*, 7626–7630.
(47) Sun, W.; Zhu, H.; Barron, P. M. Binuclear Cyclometalated Platinum(II) 4,6-Diphenyl-2,2′-bipyridine Complexes: Interesting Photoluminescent and Optical Limiting Materials. *Chem. Mater.* **2006**, *18*, 2602–2610.
(48) Lu, W.; Mi, B.-X.; Chan, M. C. W.; Hui, Z.; Che, C.-M.; Zhu, N.; Lee, S.-T. Light-Emitting Tridentate Cyclometalated Platinum(II) Complexes Containing σ-Alkynyl Auxiliaries: Tuning of Photo- and Electrophosphorescence. *J. Am. Chem. Soc.* **2004**, *126*, 4958–4971.
(49) Liu, R.; Li, Y.; Li, Y.; Zhu, H.; Sun, W. Photophysics and Nonlinear Absorption of Cyclometalated 4,6-Diphenyl-2,2′-bipyridyl Platinum(II) Complexes with Different Acetylide Ligands. *J. Phys. Chem. A* **2010**, *114*, 12639–12645.
(50) Jacquemin, D.; Perpète, E. A.; Scuseria, G. E.; Ciofini, I.; Adamo, C. TD-DFT Performance for the Visible Absorption Spectra of Organic Dyes: Conventional versus Long-Range Hybrids. *J. Chem. Theory Comput.* **2008**, *4*, 123–135.